Spaceborne SAR image geocoding with RFM model

WEI Xiaohong, ZHANG Lu, HE Xueyan, LIAO Mingsheng

State Key Laboratory of Information Engineering in Surveying, Mapping and Remote Sensing, Wuhan University, Wuhan 430079, *China*

Abstract: The methodology of RFM modeling for spaceborne SAR and its application in SAR image geocoding are investigated in this paper. The issues associated with model construction, parameter solution and refinement of RFM model are extensively studied. When the rigorous sensor model is known, a virtual control point grid can be established in a terrain-independent way for RFM modeling. A new approach is implemented to obtain unbiased solutions of RFM model parameters at a low computation time cost. The resultant RFM model can be used as a reliable substitute for the Range-Doppler (RD) model for geometric processing of SAR images as the fitting accuracy with reference to the RD model is usually better than 0.01 pixels. However, in general there will be geometric biases in the geocoded SAR images because systematic absolute geolocation errors usually exist in the RD and associated RFM models. To solve this problem, control points are used to derive an additional mathematical transformation to remove the absolute geolocation errors in the RFM model. Experimental results with ENVISAT ASAR data show the effectiveness of the proposed method for RFM model construction.

Key words: SAR, Range-Doppler, rational function model, geolocation, geocoding

CLC number: TP751.1 **Document code:** A

Citation format: Wei X H, Zhang L, He X Y and Liao M S. 2012. Spaceborne SAR image geocoding with RFM model. Journal of Remote Sensing, 16(5): 1089–1099

1 INTRODUCTION

Synthetic aperture radar (SAR) takes an imaging geometry of side-looking and ranging. As a result, the geometric distortions such as foreshortening, layover and shadow make it difficult for non-expert users to understand SAR image and to draw thematic information. Meanwhile, SAR image is usually stored in image coordinate system (azimuth line and range pixel) and must be converted into geographic coordinate system (longitude and latitude, or projection plane coordinates) before analysis and information extraction together with other geo-spatial data. Therefore, geometric correction is generally needed for SAR image analysis to eliminate geometric distortion and to convert it into geographic coordinate system for storage. The key problem for geometric correction is to determine the corresponding relationship between the ground point coordinates and the image coordinates, which is the very major function that image sensor model has realized (Fraser & Hanley, 2005).

There are mainly two types of imaging sensor models: rigorous sensor model and generic sensor model. The former usually takes collinearity equation as its theoretic basis and is able to describe the physical process of imaging completely and precisely. This model often has a complicated form, and the sensor models for different sensor types are also different in forms. Range-Doppler model (RD) is the rigorous sensor model generally adopted by mainstream space-borne SAR system. It is of high precision in geometric positioning, but the solution of its positioning is iterative and its computing efficiency is low.

The generic sensor model takes rational function model (RFM) as its typical representative. It does not need to consider the physical process of sensor imaging, but directly uses mathematical functions to describe the relationship between geographic coordinates and image coordinates. Thus it has the advantages of being simple and uniform in form and easy to realize (Hu, et al., 2004).

In operational application, the establishment of general sensor model needs to take rigorous model as the foundation and cannot be separated from the latter. The largest advantage of using generic sensor model to perform the geometric correction of image is to gain a computation efficiency that is much higher than the rigorous model. However, at present the research on the generic sensor model suitable for SAR image is limited and there are still many problems to be solved. Therefore, in this paper we studied the method of establishing RFM for SAR image, and furthermore, we realized the fast and accurate geometric correction of SAR image.

Received: 2011-09-28; **Accepted:** 2012-01-15

Foundation: The Dragon2 program (No.5297); National High Technology Research and Development Program of China (No.2011AA120404); National Natural Science Foundation of China (No.41021061); Doctoral Program Foundation of Institutions of Higher Education of China (No.20110141110057)

First author biography: WEI Xiaohong (1986—), female, master candidate, she majors in research and development of smart grid information technology. E-mail: xiaohong.wei.china@gmail.com

Corresponding author biography: ZHANG Lu (1975—), Ph.D., associate professor, his research interests are SAR remote sensing and its applications. E-mail: luzhang@whu.edu.cn

2 SENSOR MODELS FOR SAR IMAGE

As a rigorous sensor model adopted by mainstream space-borne SAR systems, the RD model is comprised of the slant range equation and the azimuth Doppler equation. When RD model is used to determine geographic coordinates for given image coordinates, the Earth ellipsoid equation is needed as an additional constrain (Hanssen & Kampes, 2008). The establishment of RD model requires accurate knowledge of satellite orbit ephemeris and SAR imaging system parameters. As the RD model is non-linear, it is impossible to obtain its analytic solution, and therefore the procedure of geometric positioning with RD model is iterative. Consequently, the computation efficiency is low. Using generic sensor model to replace RD model in the geometric correction of SAR image can effectively solve this problem and greatly improve handling efficiency.

As a generic sensor model, the RFM model has the advantages of being independent of sensor type, high fitting accuracy and being suitable for fast computation. It has been widely applied in the geometric processing of high-resolution optical image, but gains rare application in SAR image processing. In this paper, we studied the methodology of building RFM model for spaceborne SAR image, and realized the geometric correction of SAR image with RFM model.

2.1 The mathematic form of RFM model

RFM model formulates the image coordinate (r, c) as a polynomial ratio function with its corresponding geographic coordinate (P, L, H) as independent variables, shown as below.

$$\begin{cases} r = \dfrac{p_1(P,L,H)}{p_2(P,L,H)} \\ c = \dfrac{p_3(P,L,H)}{p_4(P,L,H)} \end{cases} \tag{1}$$

Eq. (1) is called the forward transformation of RFM, and the term of backward transformation refers to the conversion from image coordinate to geographic coordinate. (r, c) is the normalized image coordinate, i.e. converted the original image coordinate into the range between –1.0 and +1.0 through offset and scaling. Similarly, (P, L, H) is the normalized geographic coordinate, i.e. latitude, longitude and altitude. p_n means the numerator and denominator polynomials that constitute the ratio and its common mathematic expression is shown as below.

$$\begin{aligned} p_n(P,L,H) = \sum_{i=0}^{n_1}\sum_{j=0}^{n_2}\sum_{k=0}^{n_3} a_t P^i L^j H^k = {} & a_0 + a_1 L + a_2 P + \\ & a_3 H + a_4 PL + a_5 LH + a_6 PH + a_7 L^2 + \\ & a_8 P^2 + a_9 H^2 + a_{10} PLH + a_{11} L^3 + a_{12} P^2 L + \\ & a_{13} LH^2 + a_{14} PL^2 + a_{15} P^3 + a_{16} PH^2 + \\ & a_{17} L^2 H + a_{18} P^2 H + a_{19} H^3 \end{aligned} \tag{2}$$

where a_t (t=0, 1, ⋯, 19) is the coefficient of polynomials and called rational polynomial coefficient (RPC). To assure the model uniformity, the coefficients of constant terms in the two denominator polynomials are fixed as 1.

2.2 The general process of building RFM model

The procedure of RFM model building consists of three major steps: the establishment of virtual control point grid, the determination of RFM model parameters, and the refinement of RFM model. The third step requires using ground control points (GCPs).

2.2.1 Establishment of virtual control point grid

When the rigorous sensor model is known, the terrain-independent solution should be used. First, control points are evenly scattered across the object space covered by SAR image, and then their image coordinates are calculated using the rigorous RD model. Such control points are virtually obtained and we only need to know the rough range of altitude. For the third-order RFM model with different denominators, at least 39 control points are needed.

2.2.2 Solving RFM model parameters

The second step of building RFM model is to establish normal equation on the basis of control points and to determine the unknown model parameters through solving the normal equation. Assuming that the control grid has n points, that it to say, n observations are $\{r_i, c_i, P_i, L_i, H_i\}$ (i=1, 2, ⋯, n), respectively, then the following normal equation can be obtained by

$$\boldsymbol{\Delta} = \boldsymbol{WBX} - \boldsymbol{Wl} \tag{3}$$

where $\boldsymbol{\Delta}$ means observation error vector, and $\boldsymbol{X}$ means 78 column vector of unknown parameter to be calculated. $\boldsymbol{B}$ is the design matrix of $2n$ rows and 78 columns. $\boldsymbol{l}$ is a column vector of observed value whose size is $2n$. $\boldsymbol{W}$ is a weight matrix and is generally assumed as identity matrix which means that all observation samples have the same weight.

According to the principle of ordinary least squares adjustment, the solution can be gained as below.

$$\hat{\boldsymbol{X}} = (\boldsymbol{B}^{\mathrm{T}}\boldsymbol{WB})^{-1}\boldsymbol{B}^{\mathrm{T}}\boldsymbol{W}L \tag{4}$$

When RFM model takes the form of third-order, there are 78 unknown parameters to be solved. Therefore, the problem of over parameterization often appears, causing an extremely large conditional number of the matrix $\boldsymbol{B}^{\mathrm{T}}\boldsymbol{B}$ and thus making the normal equation become ill-conditioned.

There are primarily two kinds of solutions to ill-conditioned equation: biased ridge estimation and unbiased method of iteration by correcting characteristic value (ICCV). The basic idea of ridge estimation is to add small disturbance terms as the so-called ridge parameter to the diagonal elements of normal matrix so as to reduce or even remove the ill-condition of normal equation for the purpose of obtaining stable solution. The optimal determination of ridge parameter is the key problem for ridge estimation, and its solutions commonly used include ridge trace method, L-curve and general cross validation (GCV). The ICCV method obtains stable solution by using iterative process without changing the equality relation of normal equation. The specific technical details of these methods are described in detail in documents (Hansen, 1992; Hansen O'Leary, 1993; Golub, et al., 1979; Hanssen & Kampes, 2008; Atsushi, 1999; Toutin, 1996; Chen & Wang, 1987).

We have conducted numerous experiments on these methods and compared their advantages as well as disadvantages. The results show that ridge trace method is quite time-consuming and of low fitting accuracy. The GCV method is a bit better than the ridge trace method but its computation efficiency is comparatively low. The method of L-curve is speedy and the fitting accuracy of its solution is higher than the ridge trace and GCV methods. The unbiased ICCV method can provide the highest fitting accuracy but it

strongly depends on the initial value of solution and usually takes a long computation time. So we proposed a new approach which combines the biased L-curve ridge estimation and the unbiased ICCV method. According the new approach, a sub-optimal solution is firstly obtained by using the L-curve ridge estimation, and then the solution is provided as the initial solution for the ICCV method to start the iterations to obtain the final unbiased result. Thus, the advantages of both methods can be exploited together and the unbiased solution of high precision can be gained within a short computing time. The feasibility and effectiveness of this approach have been demonstrated in our recent study (Zhang, et al., 2011).

2.2.3 Refinement of RFM model

The objective of building RFM model is to implement a high-accuracy fitting of rigorous sensor model by the mathematical function of general form. Therefore, when rigorous model has systematic error in geometric positioning, the RFM model established will also have the same error. In order to assure the high accuracy of geometric positioning of SAR image, ground control points have to be used to carry out the refinement of RFM model and eliminate the adverse effect of such systematic error.

The refinement of RFM model usually does not directly correct RFM model's parameters, but is carried out in an indirect way. For a given ground point with known geographic coordinates, the corresponding image coordinates are firstly determined using RFM model. Then corrections will be made on the image coordinates using an additional mathematic transformation, e.g. affine transformation, to move it to the real position in image space. The parameter for the mathematic transformation is estimated from a few control points (Wang, 1987; Wang, et al., 2001).

The general form of affine transformation in image space is defined as below.

$$\begin{cases} y = e_0 + e_1 \cdot r + e_2 \cdot c \\ x = f_0 + f_1 \cdot r + f_2 \cdot c \end{cases} \tag{5}$$

where (x, y) is the measured image coordinates of control point, (r, c) is the image coordinates determined by the RFM model, e_i and f_i $(i=0,1,2)$ are the coefficients of affine transformation in image space and is estimated by using least squares adjustment. Affine transformation is a linear model, so the calculation of its parameters does not need initial values.

3 EXPERIMENTAL RESULTS AND ANALYSES

3.1 Evaluation of RFM model solution

In order to evaluate the fitting accuracy of the RFM model using the proposed method with respect to the rigorous RD model, a check point grid must be established to calculate statistical errors. The procedure of establishing check point grid is the same as that of setting up the control point grid, and they must be mutually independent. The statistical index used includes maximum absolute error (MAE) and root-mean- square error (RMSE).

Five different spaceborne SAR datasets of standard Stripmap-mode single-look complex product have been taken as test data. They cover various test areas of different terrain conditions, including Tai'an, Three Gorges and Shanghai of China, and Waterloo of Canada.

In our experiments the sizes of control point grid and check point grid were set as 10×10×7 and 20×20×14, respectively. Table 1 lists the fitting accuracies of those RFM model built with reference to the RD model. It can be seen that the RFM model can fit well to the RD model and the fitting error is usually within 0.01 pixels, implying that it can effectively replace RD model in the geometric processing of SAR image. Meanwhile, under the same experimental conditions, the fitting accuracy of RFM model in plain area is obviously better than those in mountainous area. This means that building the RFM model for SAR image of mountainous area usually requires more altitude layers than that in plain areas.

Table 1 Fitting accuracy of RFM solutions for different SAR datasets (unit: 10^{-3} pixels)

Sensor type	Region	for CNP		for CKP	
		MAE	RMSE	MAE	RMSE
ENVISAT ASAR	Tai'an, China	0.469	0.148	2.070	0.228
ALOS PALSAR	Three Gorges, China	0.122	0.078	2.860	0.434
COSMO-SkyMed	Shanghai, China	0.173	0.047	0.360	0.061
RADARSAT-2	Waterloo, Canada	0.242	0.090	0.673	0.105
TerraSAR-X	Three Gorges, China	0.267	0.122	9.000	1.890

3.2 RFM model used for geometric correction of SAR image

In this experiment the ENVISAT ASAR image covering Tai'an, China was taken as the test data. It is acquired from a descending orbit on Nov. 21st, 2004. The DEM data used for geometric correction is the freely available ASTER GDEM of 1 arc-second resolution (about 30 m) jointly released by METI and NASA.

Fig. 1 is the result of geometric correction using the RFM model. It can be seen that in the corrected image ground features such as cities, roads, mountains and rivers are clearly visible. The inherent geometric distortion characteristics in SAR image over mountainous area, such as foreshortening, layover and shadow, have been partially compensated, which is beneficial for non-expert users to understand SAR image and extract thematic information.

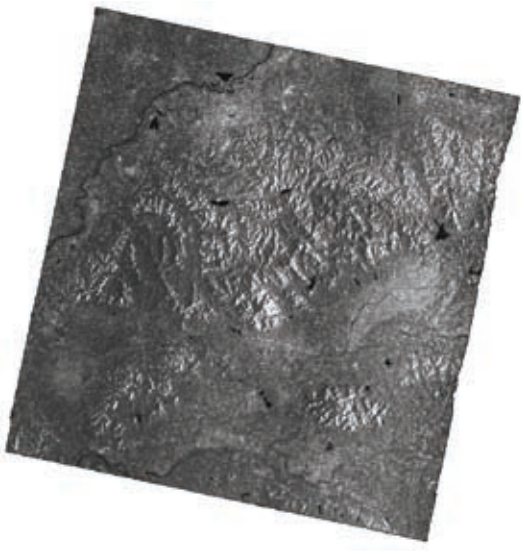

Fig. 1 Geocoded Envisat ASAR image of Tai'an, China

In addition, to quantitatively evaluate the absolute positioning accuracy of the geocoded SAR image, we carried out an analysis in which the outcome image was superimposed to an orthorectified Landsat5 TM image acquired on Sep. 23rd, 2006. It is easy to find that the result of SAR geocoding keeps a high location accuracy in the Northing direction with the error within 2 pixels, while a significant difference exists in the Easting direction with the largest error as high as 5 to 6 pixels. This is mainly due to the range propagation delay induced by atmospheric disturbances. Fig. 2 illustrates a few local areas where such difference can be seen intuitively. To eliminate this systematic error, we use a few control points to conduct refinement of the RFM model.

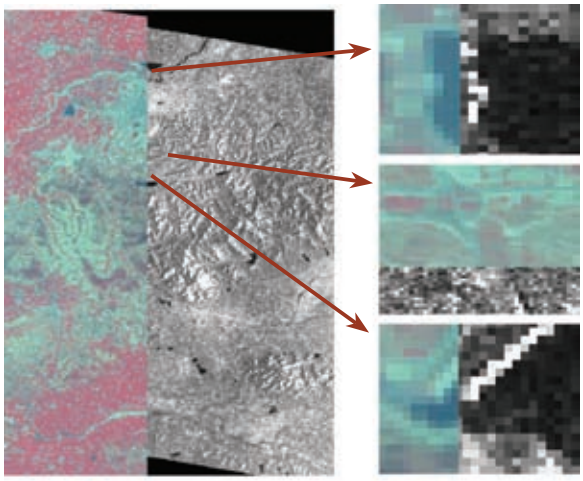

Fig. 2 The geocoded Envisat ASAR image superimposed to the orthorectified Landsat5 TM image

As there is no actually measured ground control point available, 10 pairs of tie-point were manually identified from the geocoded SAR image and TM image, and their coordinates in the two images were extracted. Then the parameters of the affine transformation model were estimated using least squares adjustment.

Fig. 3 shows the details of misalignment at two local areas before and after RFM model refinement. It is found by visual interpretation that the systematic error of RFM model has been effectively removed and a higher absolute geolocation accuracy was obtained.

In order to perform further quantitative analysis on the positioning accuracy of the geocoded SAR image, another 10 pairs of tie-points were identified from the geocoded SAR image and TM image to act as the check points. These check points were collected in the same way as that for the control points, and they were independent of each other. Fig. 4 shows the spatial distribution of all the identified tie-points. The green triangle stands for control point and the red cross points reprsent check point. Table 2 lists the WGS84/UTM coordinates and residual positioning error at the check points in the geocoded SAR images before and after model refinement with respect to the TM image.

It can be seen from Table 2 that for the geocoded SAR image before model refinement, the largest positioning errors are as high as 18 m and 154 m in Northing and Easting directions, respectively. By comparison, such errors in the geocoded SAR image after model refinement were greatly reduced to about 11 m and 28 m, respectively. Positioning accuracy was improved substantially. Thus this experiment fully states the necessity and effectiveness of carrying out refinement for the RFM model.

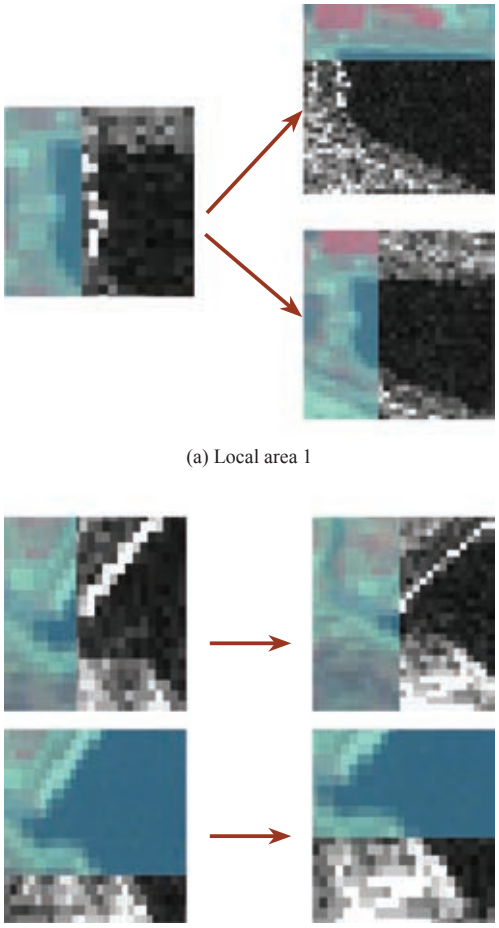

(a) Local area 1

(b) Local area 2

Fig. 3 Misalignments between geocoded SAR and TM images before and after RFM model refinement

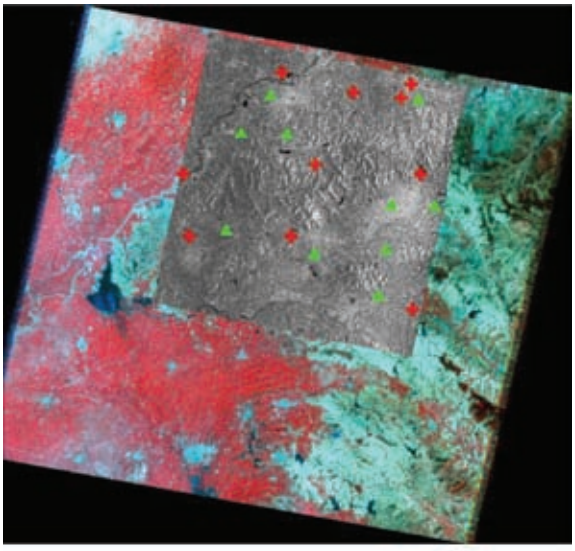

▲ Control points + Check points

Fig. 4 Distribution of control points and check points

Table 2 Comparison of geolocation accuracies before and after the refinement /m

Point index	TM image coordinate		before affine transformation				after affine transformation			
			ASAR image coordinate		Residual error		ASAR image coordinate		Residual error	
	X	*Y*	*X*	*Y*	*X*	*Y*	*X*	*Y*	*X*	*Y*
1	497389.69	4069180.31	497503.36	4069186.91	113.66	6.59	497398.95	4069191.73	9.26	11.42
2	540586.88	4058255.63	540441.68	4058269.72	–145.19	14.09	540559.23	4058244.47	–27.65	–11.15
3	545360.63	4058701.88	545514.93	4058694.29	154.31	–7.59	545371.32	4058697.45	10.69	–4.42
4	545478.75	4060886.25	545343.75	4060886.25	–135.00	0.00	545456.88	4060891.88	–21.88	5.63
5	547642.50	3975483.75	547714.40	3975496.99	71.90	13.24	547626.49	3975481.54	–16.01	–2.21
6	500906.25	4004426.25	500996.44	4004431.29	90.19	5.04	500917.95	4004431.29	11.70	5.04
7	460445.63	4004446.88	460531.52	4004437.08	85.89	–9.79	460443.60	4004448.67	–2.03	1.79
8	552255.00	4028910.00	552384.94	4028892.03	129.94	–17.97	552259.35	4028912.06	4.35	2.06
9	510461.25	4032618.75	510536.91	4032602.95	75.66	–15.80	510474.11	4032626.11	12.86	7.36
10	458135.63	4028934.38	458223.72	4028926.79	88.09	–7.59	458151.50	4028930.65	15.88	–3.73

Another fact worth pointing out is that the procedure of ASAR image geocoding only costs 4 min when using RFM model, while the computation time cost will be as high as 41 min when using the rigorous RD model.

3.3 Brief Summary

The above experimental result shows that the RFM model for spaceborne SAR image can achieve high fitting accuracy with reference to the rigorous RD model and its time cost when applied to geocoding is far less than that of using RD model. Therefore, RFM model can be used as an effective replacement of RD model and be applied in the geometric processing of spaceborne SAR images. On the other hand, as RFM model has systematic error in absolute positioning, a few ground control points are required to conduct refinement of the RFM model and thus greatly improving the absolute positioning accuracy.

4 CONCLUSIONS AND DISCUSSION

In this paper, the methodology of building RFM model for spaceborne SAR image data and its application in SAR image geocoding are investigated, and the following two conclusions are obtained:

(1) RFM model is suitable for geometric processing of spaceborne SAR images acquired by various sensors, and its planimetric fitting accuracy with respect to the rigorous RD model is usually better than 0.01 pixels. On the other hand, the computation time cost of SAR image geocoding using the RFM model is far less than that of using the RD model. Therefore, RFM model can be used as an effective replacement of RD model to be applied in the fast geometric processing of spaceborne SAR image.

(2) As the RD model usually has absolute positioning error, the RFM model built from the RD model will also have the same error, which may cause significant positioning deviation from the true geographic location in the geocoded SAR image. To solve this problem, a few control points are needed to establish an affine transformation to further refine the positioning result with the RFM model. The experimental result shows that the absolute positioning accuracy can be greatly improved with the model refinement.

However, it is noticeable that the control points in our study are chosen manually and thus they are of limited precision. If accurate measured ground control points of higher precision are available and used, the absolute positioning accuracy of the final result will be improved further.

REFERENCES

Chen X R and Wang S G. 1987. Modern Regression Analysis-Principles Methods and Applications. Hefei: Anhui Education Press

Fraser C S and Hanley H B. 2005. Bias compensated RPCs for sensor orientation of high resolution satellite imagery. Photogrammetric Engineering and Remote Sensing, 71(8): 909–915

Golub G H, Heath M and Wahba G. 1979. Generalized cross-validation as a method for choosing a good ridge parameter. Technometrics, 21(2): 215–223 [DOI: 10.2307/1268518]

Hansen P C. 1992. Analysis of discrete ill-posed problems by means of the L-curve. SIAM Review, 34(4): 561–580 [DOI: 10.1137/1034115]

Hansen P C and O'Leary D P. 1993. The use of the L-curve in the regularization of discrete ill-posed problems. SIAM Journal on Scientific Computing, 14(6): 1487–1503 [DOI: 10.1137/0914086]

Hanssen R and Kampes B. 2008. Delft Object-Oriented Radar Interferometric Software User's Manual and Technical Documentation. Delft University of Technology

Hu Y, Tao V and Croitoru A. 2004. Understanding the rational function model: methods and applications. International Archives of the Photogrammetry, Remote Sensing and Spatial Information Sciences, 35(Part B4): 663–668

Okamoto A. 1999. Geometric characteristics of alternative triangulation models for satellite imagery // ASPRS 1999 Annual Conference Proceedings. Oregon, USA: 64–72

Toutin T. 1996. Opposite side ERS-1 SAR stereo mapping over rolling topography. IEEE Transactions on Geoscience and Remote Sensing, 34(2): 543–549 [DOI: 10.1109/36.485130]

Wang S G. 1987. Linear Model Theory and Its Applications. Hefei: Anhui Education Press

Wang X Z, Liu D Y, Zhang Q Y and Huang H L. 2001. The iteration by correcting characteristic value and its application in surveying data processing. Heilongjiang Institute of Technology, 15(2): 3–6.

Zhang L, He X Y, Balz T, Wei X H and Liao M S. 2011. Rational function modeling for spaceborne SAR datasets. ISPRS Journal of Photogrammetry and Remote Sensing, 66(1): 133–145 [DOI: 10.1016/j.isprsjprs.2010.10.007]

基于有理函数模型的星载SAR影像几何校正

魏晓红，张路，贺雪艳，廖明生

武汉大学 测绘遥感信息工程国家重点实验室，湖北 武汉 430079

摘 要：主要研究了面向星载合成孔径雷达SAR（Synthetic Aperture Radar）影像几何处理的有理函数模型RFM（Rational Function Model）的建模、求解和应用方法。首先采用与地形无关的方式，利用严密的距离-多普勒模型（Range-Doppler，RD）构建虚拟控制点格网来进行RFM建模，实现了一种RFM模型参数的快速无偏解算新方法，能够取得相对于RD模型很高的拟合精度，在几何定位功能上实现了对RD模型的有效替代，同时大大提高了计算效率。然后在此基础上利用RFM模型实现了星载SAR影像的快速几何校正，为了提高几何校正结果的绝对定位精度，引入少量地面控制点对RFM模型进行了像方改正处理，以消除SAR影像几何定位的系统误差，并利用ENVISAT ASAR数据的实验结果验证了本文方法的有效性。

关键词：合成孔径雷达，距离-多普勒模型，有理函数模型，几何定位，几何校正

中图分类号：TP751.1 **文献标志码**：A

引用格式：魏晓红，张路，贺雪艳，廖明生．2012．基于有理函数模型的星载SAR影像几何校正．遥感学报，16(5): 1089–1099
Wei X H, Zhang L, He X Y and Liao M S. 2012. Spaceborne SAR image geocoding with RFM model. Journal of Remote Sensing, 16(5): 1089–1099

1 引 言

合成孔径雷达采用侧视距离成像方式，由此带来的透视收缩、叠掩和阴影等几何畸变特征对于一般用户理解SAR影像并从中提取专题信息造成了困难。同时，SAR影像通常按照影像行列坐标(方位向加距离向)存储，必须转换到地理坐标系(经纬度或投影平面坐标)下，才能与其他空间数据开展联合分析和信息提取。因此，SAR影像分析一般需要对其进行几何校正处理，消除几何畸变并变换到地理坐标系存储。几何校正的核心问题是确定描述地面点坐标与影像行列坐标之间的对应关系，这正是成像传感器模型实现的主要功能(Fraser和Hanley, 2005)。

成像传感器模型主要分为两大类：严密传感器模型和通用传感器模型。前者通常以共线方程为理论基础，能够完整准确地描述成像物理过程，模型形式复杂，并且不同类型的传感器所对应传感器模型形式也不相同。RD模型是主流星载SAR系统普遍采用的严密传感器模型，其几何定位精度高，但定位过程需迭代求解，计算效率较低。后者以RFM模型为典型代表，它不需要考虑传感器成像的物理过程，直接采用数学函数来描述地面点和相应像点坐标之间的对应关系，具有形式简单统一、易于实现的优点(Hu 等, 2004)。

在实际应用中，通用传感器模型的建立一般需要以严密模型为基础，不能脱离后者独立存在。采用通用传感器模型进行影像几何校正最大的好处是可以获得远高于严密模型的计算效率。然而，目前对于适用于SAR影像的通用传感器模型研究还不多，还有不少问题有待解决。因此，本文研究了面向SAR影像的有理函数模型的建立求解方法，在此基础上实现了SAR影像的快速高精度几何校正处理。

收稿日期：2011-09-28；**修订日期**：2012-01-15

基金项目：中欧科技合作“龙计划”二期项目(编号: 5297)；国家高技术研究发展计划(863计划)(编号: 2011AA120404)；国家自然科学基金(编号: 41021061)；高等学校博士学科点专项科研基金(编号: 20110141110057)

第一作者简介：魏晓红(1986—)，女，硕士，现从事智能电网方面的研究，已发表论文3篇。E-mail: xiaohong.wei.china @gmail.com。

通信作者简介：张路(1975—)，男，博士，副教授，主要从事雷达遥感及其应用研究。E-mail: luzhang@whu.edu.cn。

2 SAR影像传感器模型

RD模型是由距离向上的斜距方程和方位向上的多普勒方程构成，在用于从像点坐标确定地面点坐标时还需要加上地球椭球方程(Hanssen和Kampes, 2008)。RD模型的构建需要详细的卫星轨道星历和SAR成像系统参数，形式较为复杂，利用其进行几何定位需要迭代解算，计算效率不高。采用通用传感器模型来替代RD模型用于SAR影像几何校正，可以有效解决这一问题，大幅提高处理效率。

RFM模型作为一种通用传感器模型，具有与传感器无关、拟合精度高、计算速度快等优点，已经在高分辨率光学影像几何处理方面得到了广泛应用，但在SAR影像几何处理方面还很少应用。鉴于此，本文研究了适用于星载SAR影像的RFM模型的构建求解问题，并实现了基于RFM模型的SAR影像几何校正。

2.1 RFM模型的数学形式

RFM模型将像点坐标(r, c)表示为以其相应地面点坐标(P, L, H)为自变量的多项式比值函数，如式(1)所示：

$$\begin{cases} r = \dfrac{p_1(P,L,H)}{p_2(P,L,H)} \\ c = \dfrac{p_3(P,L,H)}{p_4(P,L,H)} \end{cases} \tag{1}$$

式(1)为RFM的正变换形式，而由影像坐标到地面点坐标的转换是反变换形式。式中，(r, c)为归一化的影像坐标，即将每个影像像元的行列号通过偏移和缩放等处理变换到–1.0和+1.0之间，(P, L, H)为归一化的地面点坐标，即经度、纬度和高程。p_n表示构成比值的分子和分母多项式，其数学表达形式如下：

$$\begin{aligned} p_n(P,L,H) = \sum_{i=0}^{n_1}\sum_{j=0}^{n_2}\sum_{k=0}^{n_3} a_t P^i L^j H^k = {} & a_0 + a_1 L + a_2 P + \\ & a_3 H + a_4 PL + a_5 LH + a_6 PH + a_7 L^2 + \\ & a_8 P^2 + a_9 H^2 + a_{10} PLH + a_{11} L^3 + a_{12} P^2 L + \\ & a_{13} LH^2 + a_{14} PL^2 + a_{15} P^3 + a_{16} PH^2 + \\ & a_{17} L^2 H + a_{18} P^2 H + a_{19} H^3 \end{aligned} \tag{2}$$

式中，a_t (t=0, 1, …, 19)是多项式的系数，称为有理函数系数RPC(Rational Polynomial Coefficient)。为保证模型形式的一致性，两个分母多项式中的常数项系数固定取值为1。

2.2 RFM建模的一般流程

RFM模型的建立过程包括3个主要步骤：控制点格网的建立，RFM模型参数的求解和RFM模型的像方改正。其中，RFM模型的像方改正需要使用地面控制点GCPs。

2.2.1 建立控制点格网

在严密成像模型已知的情况下，采用地形无关的求解方式。首先在影像覆盖的物方空间范围内按不同的高程分层设立控制点集合，并通过严密的RD模型求解对应的影像坐标。这种方法中控制点是虚拟的，只需要高程取值范围信息。对于常用的三阶分母不同的RFM模型，最少需要39个控制点。

2.2.2 RFM模型参数求解

在控制点集合的基础上建立法方程，通过求解法方程确定未知参数RPC。假设控制格网有n个点，也就是说，n个观测量分别为$\{r_i, c_i, P_i, L_i, H_i\}$($i$=1, 2, …, n)，则可得到法方程如下式：

$$\boldsymbol{\Delta} = \boldsymbol{WBX} - \boldsymbol{Wl} \tag{3}$$

式中，$\boldsymbol{\Delta}$表示观测误差向量，$\boldsymbol{X}$表示待求的78个未知参数列向量。$\boldsymbol{B}$是大小为2n行78列的系数矩阵，$\boldsymbol{l}$是大小为2n的观测值列向量，$\boldsymbol{W}$为权矩阵，一般设为单位阵，表示各观测样本权重相同。

根据经典的最小二乘平差原理得到法方程的解：

$$\hat{\boldsymbol{X}} = (\boldsymbol{B}^{\mathrm{T}}\boldsymbol{WB})^{-1}\boldsymbol{B}^{\mathrm{T}}\boldsymbol{W}L \tag{4}$$

当RFM模型采用三阶形式时，需要解算的未知参数有78个，在解算其模型参数时，往往存在过度参数化的问题，致使法矩阵$\boldsymbol{B}^{\mathrm{T}}\boldsymbol{B}$的条件数变得非常大，上述最小二乘解就会不稳定，导致得到的模型具有很大的拟合误差。因此，解决病态方程问题是求解RFM模型参数的关键。

病态方程的传统求解方法主要有两类：有偏的岭估计法和无偏的谱修正迭代法。岭估计法的基本思想是对法矩阵的对角线元素加上称之为岭参数的微小扰动项，从而减小甚至消除法方程的病态性，达到获得稳定解的目的。岭参数的优化确定是岭估计法的核心问题，常用解决方法包括岭迹法、L曲线法和广义交叉验证法。谱修正迭代法则是在不改变法方程等式关系的前提下，采用迭代过程逼近得到稳定无偏解。这几种方法的具体技术细节参考以下文献(Hansen，

1992；Hansen和O'Leary，1993；Golub 等，1979；Hanssen和Kampes，2008；Okamoto，1999；Toutin，1996；陈希孺和王松桂，1987)。

我们对这些方法进行了大量实验，比较了它们的优缺点。实验结果表明，岭迹法相当费时且精度不高，广义交叉验证法精度略优于岭迹法但计算速度仍较慢，L曲线法速度很快，精度也高于岭迹法和广义交叉验证法，谱修正迭代法的结果精度最高，但其极度依赖初值的迭代过程需花费大量计算时间。因此，我们提出实现了一种利用L曲线岭估计和谱修正迭代法相结合的新方法，首先采用L曲线岭估计法得到近似最优解，然后以其作为谱修正迭代的初值，迭代逼近得到最终结果。这样，两种方法的优点可以结合起来，耗费很少的计算时间得到高精度的无偏解。这种方法的可行性和有效性在我们之前的研究中已得到证实(Zhang 等，2011)。

2.2.3 RFM模型的像方改正

RFM模型的本质是以通用形式数学函数实现对严密成像传感器模型的高精度拟合，因此当严密模型存在系统性的几何定位误差时，所建立的RFM模型也会具有同样的误差。为了保证SAR影像几何校正结果具有较高的精度，须采用地面控制点来对RFM模型进行像方改正，消除这种系统误差的不利影响。这些地面控制点必须独立于解求RFM模型时所使用的控制点。

RFM模型的像方改正过程不是直接修正RFM模型参数，而是对RFM模型计算得出的像方坐标，采用一个附加的数学变换，例如仿射变换来改正到其真实的像点坐标上，这一数学变换的变换参数通过少量地面控制点来估计得到(王松桂，1987；王新洲 等，2001)。

在影像像方空间上定义仿射变换：

$$\begin{cases} y = e_0 + e_1 \cdot r + e_2 \cdot c \\ x = f_0 + f_1 \cdot r + f_2 \cdot c \end{cases} \tag{5}$$

式中，(x, y)是控制点在影像上的量测坐标，(r, c)为根据RFM模型由控制点物方坐标计算得到的像方坐标，e_i和$f_i(i=0,1,2)$为待求的影像面仿射变换参数，采用最小二乘平差求解得到。仿射变换为线性模型，因此求解参数不需要初值。

3 实验结果与分析

3.1 RFM模型参数求解精度评定

为评价本文建立的RFM模型相对于严密的RD模型的拟合精度，建立检查点格网来计算统计误差。检查点格网的建立方法与RFM建模所用控制点格网相同，二者相互独立。使用的统计评价指标包括最大绝对值误差MAE和均方根误差RMSE。

该组实验使用了5种不同的星载SAR数据，均为条带模式单视复数SLC影像产品。实验区地形既有平原又有山区，地域分别为中国的泰安、三峡、上海和加拿大的滑铁卢。

实验采用控制点格网10 × 10 × 7(水平格网大小为10 × 10，高程分层为7层)，检查点格网为20 × 20 × 14。表1列出了各种不同数据求解出的RFM模型参数相对于RD模型的拟合精度。从表中可以看出，RFM模型对RD模型具有很好的拟合精度，误差都在0.01个像素之内，可以有效替代RD模型用于SAR影像几何处理。同时，在同样的实验条件下，平原地区的RFM模型拟合精度明显优于山区，这意味着山区SAR影像的RFM建模通常需要使用比平原地区更多的高程分层数。

表1 不同SAR影像数据的RFM模型的拟合精度/(10^{-3}像元)

星载SAR传感器	成像区域	控制点		检查点	
		MAE	RMSE	MAE	RMSE
ENVISAT ASAR	中国泰安	0.469	0.148	2.070	0.228
ALOS PALSAR	中国三峡	0.122	0.078	2.860	0.434
COSMO-SkyMed	中国上海	0.173	0.047	0.360	0.061
RADARSAT-2	加拿大滑铁卢	0.242	0.090	0.673	0.105
TerraSAR-X	中国三峡	0.267	0.122	9.000	1.890

3.2 用RFM模型进行SAR影像几何校正实验

实验选取覆盖中国泰安的Envisat ASAR影像作为实验数据，成像模式为IMS，成像日期为2004-11-21。用于几何校正的DEM数据为ERSDAC和NASA免费发布的1弧秒分辨率(约30 m)的ASTER GDEM。

图1是实验数据经过基于RFM模型几何校正的结果，可以看到校正后的影像中城市、道路、山体和河流等清晰可见，SAR影像在山区固有的透视收缩、叠掩和阴影等几何畸变特征得到了有效的处理，透视收缩和叠掩现象在距离向上得到了充分的拉伸，有利于一般用户对影像的理解与专题信息的提取。

此外，为了定量评价RFM模型几何校正结果的绝对定位精度，我们将这幅结果影像与同地区2006-09-23获取的Landsat5 TM正射影像进行了叠加分析。

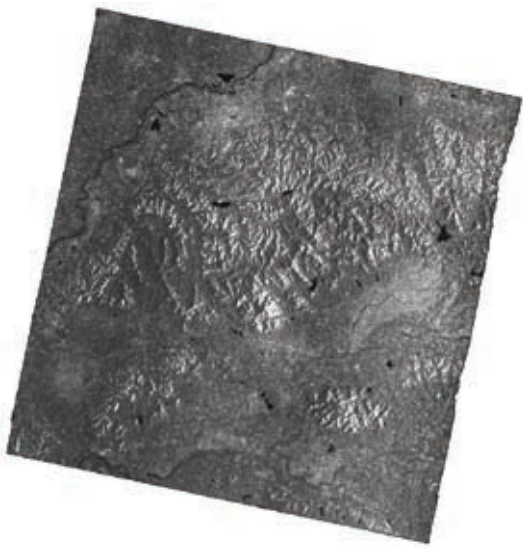

图1 泰安Envisat ASAR影像几何校正结果

不难发现，RFM模型几何校正结果在行方向上保持了很高的精度，误差一般在一两个像元之内，而在列方向上则有明显的差异，差异最大的地区可达到5、6个像元。这可能主要是由于距离向上的大气传播延迟影响所致。图2给出了局部细节图，可以直观地看到这种差异。为消除这种系统性误差，我们采用控制点对RFM模型进行像方改正的方法解决。另外，这幅影像用RFM进行几何校正处理仅仅用了4 min，与使用严密的RD模型处理耗费的41 min形成了鲜明对比。

RFM的精纠正需要控制点来求仿射变换参数，因为无实测地面控制点数据，本文采用手工选点方式选取了10个同名点作为控制点，在TM正射影像上和原始ASAR影像上分别读取它们的经纬度和行列号，由经纬度和DEM高程根据RFM模型求解校正后的影像行列号，此行列号与实际的原始影像行列号存在偏差，以这些点为基础建立仿射变换方程，采用最小二乘法求得仿射变换参数。

图3列出了像方改正前后的两处局部细节对比图。目视判读发现，经过像方改正可以有效去除RFM模型的系统误差，得到较高的绝对校正精度。

为了进一步定量分析经过RFM模型几何校正的结果SAR影像的定位精度，我们以TM正射影像作为参照，从中选取了10个同名地物点来进行检查比较。图4是这些同名点的位置分布图。表2列出了像方改正前后SAR几何校正影像与TM正射影像的同名点的WGS84/ UTM坐标和定位残差。

从表2中可以看到，像方改正前的几何校正影像相对于TM正射影像，在行方向上最大定位误差为

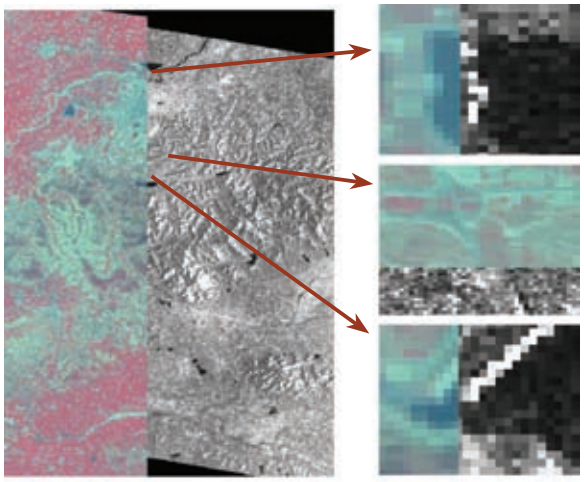

图2 Envisat ASAR校正影像与Landsat5 TM正射影像叠加图与局部细节图

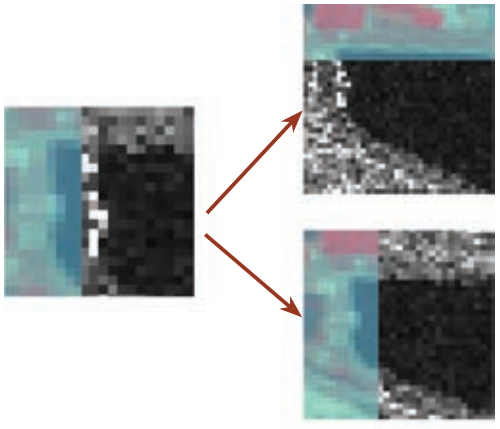

(a) 局部区域1

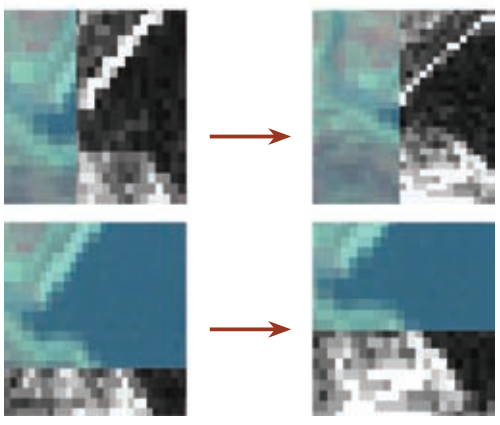

(b) 局部区域2

图3 相同局部区域像方校正前后的细节对比图

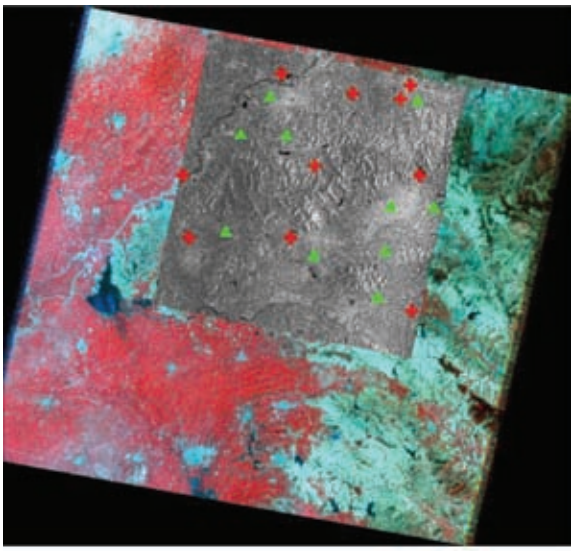

▲ 控制点 ✚ 检查点

图4 精度评定选取检查点分布图

18 m，列方向的最大误差约为154 m，在列方向上存在较大的系统误差。经过像方改正后，在行方向上的最大误差减小为11 m，列方向上的最大误差则大幅降低到约28 m，定位精度明显提高。由此充分说明了对RFM模型进行像方改正的必要性和有效性。

3.3 小结

上述实验结果表明，星载SAR影像的RFM模型对RD模型具有很高的拟合精度，并且在应用于几何校正时所花费的时间要远远小于RD模型，因此RFM模型可作为对RD模型的一种有效替代。另一方面，由于RFM模型存在系统误差，所以需要引入少量地面控制点对RFM模型进行像方改正，从而显著提高几何校正结果影像的绝对定位精度。

4 结 论

本文对RFM模型应用于SAR影像数据几何处理的方法及应用进行研究，得出以下两点结论：

表2 像方改正前后几何校正SAR影像定位精度评价结果 /m

编号	TM正射影像坐标		像方改正前				像方改正后			
			ASAR影像坐标		残余误差		ASAR影像坐标		残余误差	
	X	*Y*	*X*	*Y*	*X*	*Y*	*X*	*Y*	*X*	*Y*
1	497389.69	4069180.31	497503.36	4069186.91	113.66	6.59	497398.95	4069191.73	9.26	11.42
2	540586.88	4058255.63	540441.68	4058269.72	−145.19	14.09	540559.23	4058244.47	−27.65	−11.15
3	545360.63	4058701.88	545514.93	4058694.29	154.31	−7.59	545371.32	4058697.45	10.69	−4.42
4	545478.75	4060886.25	545343.75	4060886.25	−135.00	0.00	545456.88	4060891.88	−21.88	5.63
5	547642.50	3975483.75	547714.40	3975496.99	71.90	13.24	547626.49	3975481.54	−16.01	−2.21
6	500906.25	4004426.25	500996.44	4004431.29	90.19	5.04	500917.95	4004431.29	11.70	5.04
7	460445.63	4004446.88	460531.52	4004437.08	85.89	−9.79	460443.60	4004448.67	−2.03	1.79
8	552255.00	4028910.00	552384.94	4028892.03	129.94	−17.97	552259.35	4028912.06	4.35	2.06
9	510461.25	4032618.75	510536.91	4032602.95	75.66	−15.80	510474.11	4032626.11	12.86	7.36
10	458135.63	4028934.38	458223.72	4028926.79	88.09	−7.59	458151.50	4028930.65	15.88	−3.73

(1)RFM模型能够适用于各种星载SAR传感器获取的影像，其相对于严密RD模型的平面拟合精度均优于0.01个像元，当应用于SAR影像几何校正时RFM模型所花费的计算时间远远少于RD模型，因此RFM模型可作为RD模型的一种有效替代用于星载SAR影像的快速几何处理。

(2)在RD模型本身存在绝对定位误差的情况下，以RD模型为基础建立的RFM模型也存在相同的误差，这会使得SAR影像几何校正结果偏离真实地理位置。因此需要引入少量地面控制点，采用附加数学变换对RFM模型进行像方改正。实验结果表明，经过像方改正后的RFM模型的绝对定位精度能够得到显著提高。

本文实验研究中控制点为人工目视解译选取，

精度有限，如果采用更高精度的实测地面控制点，将会进一步提高像方改正后几何校正结果的绝对定位精度。

参考文献(References)

陈希孺, 王松桂. 1987. 近代回归分析-原理方法及应用. 合肥: 安徽教育出版社

Fraser C S and Hanley H B. 2005. Bias compensated RPCs for sensor orientation of high resolution satellite imagery. Photogrammetric Engineering and Remote Sensing, 71(8): 909–915

Golub G H, Heath M and Wahba G. 1979. Generalized cross-validation as a method for choosing a good ridge parameter. Technometrics, 21(2): 215–223 [DOI: 10.2307/1268518]

Hansen P C. 1992. Analysis of discrete ill-posed problems by means of the L-curve. SIAM Review, 34(4): 561–580 [DOI: 10.1137/1034115]

Hansen P C and O'Leary D P. 1993. The use of the L-curve in the regularization of discrete ill-posed problems. SIAM Journal on Scientific Computing, 14(6): 1487–1503 [DOI: 10.1137/0914086]

Hanssen R and Kampes B. 2008. Delft Object-Oriented Radar Interferometric Software User's Manual and Technical Documentation. Delft University of Technology

Hu Y, Tao V and Croitoru A. 2004. Understanding the rational function model: methods and applications. International Archives of the Photogrammetry, Remote Sensing and Spatial Information Sciences, 35(Part B4): 663–668

Okamoto A. 1999. Geometric characteristics of alternative triangulation models for satellite imagery // ASPRS 1999 Annual Conference Proceedings. Oregon, USA: 64–72

Toutin T. 1996. Opposite side ERS-1 SAR stereo mapping over rolling topography. IEEE Transactions on Geoscience and Remote Sensing, 34(2): 543–549 [DOI: 10.1109/36.485130]

王松桂. 1987. 线性模型的理论及其应用. 合肥: 安徽教育出版社

王新洲, 刘丁酉, 张前勇, 黄海兰. 2001. 谱修正迭代法及其在测量数据处理中的应用. 黑龙江工程学院学报, 15(2): 3–6

Zhang L, He X Y, Balz T, Wei X H and Liao M S. 2011. Rational function modeling for spaceborne SAR datasets. ISPRS Journal of Photogrammetry and Remote Sensing, 66(1): 133–145 [DOI: 10.1016/j.isprsjprs.2010.10.007]